IOP Publishing and International Atomic Energy Agency Nuclear Fusion
Nucl. Fusion **48** (2008) 115008 (11pp) doi:10.1088/0029-5515/48/11/115008

Comprehensive simulation of vertical plasma instability events and their serious damage to ITER plasma facing components

A. Hassanein and T. Sizyuk

School of Nuclear Engineering, Purdue University, 400 Central Drive, West Lafayette, IN 47907, USA

E-mail: hassanein@purdue.edu

Received 21 February 2008, accepted for publication 5 September 2008
Published 29 September 2008
Online at stacks.iop.org/NF/48/115008

Abstract
Safe and reliable operation is still one of the major challenges in the development of the new generation of ITER-like fusion reactors. The deposited plasma energy during major disruptions, edge-localized modes (ELMs) and vertical displacement events (VDEs) causes significant surface erosion, possible structural failure and frequent plasma contamination. While plasma disruptions and ELM will have no significant thermal effects on the structural materials or coolant channels because of their short deposition time, VDEs having longer-duration time could have a destructive impact on these components. Therefore, modelling the response of structural materials to VDE has to integrate detailed energy deposition processes, surface vaporization, phase change and melting, heat conduction to coolant channels and critical heat flux criteria at the coolant channels. The HEIGHTS 3D upgraded computer package considers all the above processes to specifically study VDE in detail. Results of benchmarking with several known laboratory experiments prove the validity of HEIGHTS implemented models. Beryllium and tungsten are both considered surface coating materials along with copper structure and coolant channels using both smooth tubes with swirl tape insert. The design requirements and implications of plasma facing components are discussed along with recommendations to mitigate and reduce the effects of plasma instabilities on reactor components.

PACS numbers: 52.40

1. Introduction

Deposition of powerful plasma and particle beams (power densities up to hundreds of GW m^{-2} and time duration up to tens of milliseconds) on various materials significantly damages exposed surfaces and indirectly nearby components. Detailed investigation of material erosion and damage due to intense energy deposition on target surfaces is important for many applications such as space studies, the study of earth surface interaction with colliding asteroids and comets, dense plasma sources, high-energy physics applications, thermonuclear and inertial fusion studies. An important application of this understanding is in future tokamak fusion devices during plasma transients and the resulting interaction with plasma facing materials (PFMs).

Various kinds of damage to PFM as a result of plasma instabilities still remain a major obstacle to a successful tokamak reactor design. Loss of plasma confinements and instabilities take various forms, such as major disruptions, which include both thermal and current quench (sometimes producing runaway electrons); edge-localized modes (ELMs) and vertical displacement events (VDEs). The overall damage depends on the detailed physics of plasma instabilities, the physics of plasma/material interactions and the design configuration of plasma facing components (PFCs) [1]. Most plasma instabilities such as disruptions, ELM and VDE will cause both surface and bulk damage to plasma facing and structural materials. Surface damage consists mainly of high erosion losses attributable to surface vaporization, spallation and melt layer erosion. Major bulk damage of plasma instabilities, particularly those of longer duration, such as VDE, or those with deeper deposited energy, such as runaway electrons, is the result of the high heat flux reaching the coolant channels, possibly causing burnout of these tubes [2–4]. Additional bulk damage may include large temperature increases in structural materials and at the

interfaces between surface coatings and structural materials. These large temperature increases can cause high thermal stresses, melting and detachment of surface coating material and material fatigue and failure. In addition to these effects, the transport and redeposition of the eroded surface materials to various locations on PFC are of major concern for plasma contamination, safety (dust inventory hazard) and successful and prolonged plasma operation after instability events [5].

Plasma facing surfaces are rapidly heated during plasma instabilities by the direct impact of energetic plasma particles and radiation. The deposited energy in the bulk material is calculated using models that include the physics of energy loss by plasma ions and electrons in target materials. The HEIGHTS package calculates, in detail, the spatial and time dependence of beam energy deposition in various target materials. Analytical, semi-empirical and Monte Carlo techniques were used for accurate prediction of energy deposition. In most cases, the deposited plasma energy can be high enough to rapidly melt and vaporize the surface material. The thermal response of the material is calculated by solving a multidimensional (up to 3D) time-dependent heat-conduction equation, with moving boundaries, i.e. the receding eroded surface and the solid–liquid interface, with boundary conditions that include heats of melting and vaporization [3]. Most of the calculations presented in this study are fully 3D time-dependent analysis.

In this particular study it is shown that vapour flux from the coating surface material can remove a significant part of the incident plasma energy and therefore, protect the copper substrate from overheating. The upgraded HEIGHTS simulation package is now used to simulate in full three-dimensional configurations the response of an entire ITER-like module to a VDE. Melting and vaporization of PFCs were calculated, in detail, as well as the heat fluxes from PFC to Cu coolant tubes having cylindrical geometry. A typical ITER-like VDE will have an incoming energy of 6 kJ cm^{-2} deposited in 0.5 s (i.e. VDE power of 120 MW m^{-2}). The initial temperature distribution of the PFC and the bulk substrate prior to the VDE is calculated according to steady-state heat flux, module design and initial coolant temperature. The models used in the upgraded HEIGHTS were recently benchmarked against various VDE simulation experiments using powerful electron beams and have excellent agreement with the data. Benchmarking of recent VDE data in current tokamak machines is also in good agreement with HEIGHTS.

2. Effects of longer-duration VDE plasma instabilities

The strongly elongated plasma configuration in ITER-like devices ($\kappa \approx 2$) is vertically unstable unless an active control feedback at the vertical position is applied. A malfunction of this feedback system for a variety of reasons can lead to a rapid plasma vertical displacement at full plasma current. As the plasma contacts the PFC at the top or bottom of the vacuum vessel, the current is rapidly forced to zero, similar to the behaviour of the plasma after the thermal quench of a disruption. This phenomenon constitutes the VDEs. The thermal energy of the plasma is expected to be lost at the contact point. The area of strong wall contact with the plasma will absorb a considerable fraction of the total plasma energy and can result in melting and vaporization of the PFC as well as melting of the copper substrate and burnout of coolant channels that could be a serious concern.

Usually during the early stage of any intense and short power deposition on target materials such as during a disruption or a giant ELM, a vapour cloud from the target debris will form above the bombarded surface. This shielding vapour layer, if well confined, will significantly reduce the net energy flux to the originally exposed target surface to only a few per cent of its initial incident value, thereby substantially reducing the net vaporization rate [3, 6]. In this case, most of the incident plasma energy is reradiated to nearby surfaces and components, and little energy is conducted away from the surface to the bulk structure. Both plasma disruptions and ELM have no significant thermal effect on structural materials or coolant channels due to the short deposition time (<10 ms). However, VDE (duration 100–500 ms), and runaway electrons (deeper penetration depth), do not produce an intense localized vapour cloud capable of stopping the incident plasma particles and re-radiating the incident plasma energy. Therefore, VDE and runaway electrons, in addition to causing severe surface melting and erosion, can substantially damage the structural materials and coolant channels [3]. The concern is the higher temperatures observed in the structural material, particularly at the interface with the coating materials. These high temperatures and thermal stresses in the structure can seriously degrade the integrity of the interface bonding; this may lead to detachment of the coating from the structural material. The analysis presented is for modules of both beryllium and tungsten as coating materials over copper structure with copper coolant channel. Low-z materials such as beryllium and carbon are still preferred for first wall coating/tile design while tungsten is preferred for the baffle/dome region since it can withstand higher heat fluxes and has low sputtering yield.

3. Heat transfer processes in structural materials

The heat removal from the PFC is achieved through channels with a forced flow of sub-cooled liquid, using the heat transfer principle of sub-cooled boiling. Under sub-cooled boiling, the bulk liquid temperature in the channels can be significantly lower than the saturation temperature. Accordingly, the contribution of single-phase forced convection to the heat exchange is considerable. Since the channel wall temperature is lower than saturation temperature, the heat transfer is determined only by the single-phase forced convective heat exchange mechanism. Nucleate boiling processes at the channel wall are possible if the wall temperature exceeds the saturation temperature by some value. In this case vapour bubbles are formed on the internal channel surfaces, rushed into the bulk liquid and condensed. As the temperature difference increases, nucleate boiling plays a more important role in the heat transport. At this stage bubbles accumulation and condensation rate at the wall surface will increase. As a result, thin elongated bubbles and then a denser vapour blanket are formed at the internal wall surface. This makes it difficult for the liquid to efficiently remove the heat and therefore the heat transfer from the wall is rapidly decreased. As a result, the wall temperature is significantly increased [7]. The value

of the heat flux at which this situation occurs is known as the critical heat flux (CHF). If the coolant has high mass velocity and the bulk liquid temperature is much lower than the saturation temperature, film boiling will occur where the fluid core consists of sub-cooled liquid and is isolated from the wall by a thin vapour film. The maximum wall temperature will depend on the heat flux, coolant velocity, pressure and bulk temperature. In the case of sub-cooled boiling the CHF is high; therefore the expected wall temperatures to reach the CHF are usually comparable to the melt temperature of the channel wall.

4. Mathematical model

The time-dependent heat conduction equation in 3D Cartesian coordinates (x, y, z) is given by

$$\rho c \frac{\mathrm{D}T}{\mathrm{D}t} = \frac{\partial}{\partial x}\left(\kappa(x,y,z,T)\frac{\partial T}{\partial x}\right) + \frac{\partial}{\partial y}\left(\kappa(x,y,z,T)\frac{\partial T}{\partial y}\right) + \frac{\partial}{\partial z}\left(\kappa(x,y,z,T)\frac{\partial T}{\partial z}\right) + Q(x,y,z,t), \quad (1)$$

where ρ is the density, c is the specific heat, T is the temperature, t is the time and κ is the thermal conductivity.

In the case of PFC surface, the volumetric energy deposition rate $Q(x, y, z, t)$ depends on the deposited plasma heat energy (Q_{in}) and the energy loss due to evaporation (Q_{vapour}):

$$Q(x,y,t) = Q_{\mathrm{in}}(x,y,t) - Q_{\mathrm{vapour}}(V_{\mathrm{surface}}), \quad (2)$$

where V_{surface} is the velocity of the receding surface as a result of the evaporation process. The surface velocity is given by [8, 9] (we use Gaussian units unless otherwise indicated)

$$V_{\mathrm{surface}}(x,y,t) = 5.8\times10^{-2}\frac{\alpha\sqrt{A}P_{\mathrm{v}}(T_{\mathrm{v}})}{\rho(T_{\mathrm{v}})\sqrt{T_{\mathrm{v}}}} \times[0.8+0.2\exp(-t/10\tau_{\mathrm{c}})], \quad (3)$$

where α is the sticking probability (usually $\approx$1); A is the atomic mass number of the target material; P_{v} is the vapour pressure; T_{v} is the vapour temperature and τ_{c} is the above-surface vapour collision time.

The heat exchange with sub-cooled water in the present model is described by the following processes:

- Heat transfer to the coolant is determined only by forced convection—laminar or turbulent flow (wall temperature T_{w} is less than the temperature of the onset of nucleate boiling).
- Heat transfer to the coolant depends on forced convection and nucleate boiling at the wall surface (T_{w} reaches or exceeds the value at onset of nucleate boiling).
- If the heat transfer, provided by the above processes, exceeds a critical value for given coolant conditions, heat transfer is then determined as part of the critical value (transition regime in boiling curve).

Figure 1 illustrates the different regimes of heat flux to the coolant in dependence on the wall temperature.

Detailed film boiling processes are not considered in this paper since copper is considered the coolant wall material. Copper has low melt temperature, comparable to the temperature of film boiling onset [10], therefore the copper wall will melt and be destroyed before a stable film boiling in the channel will occur.

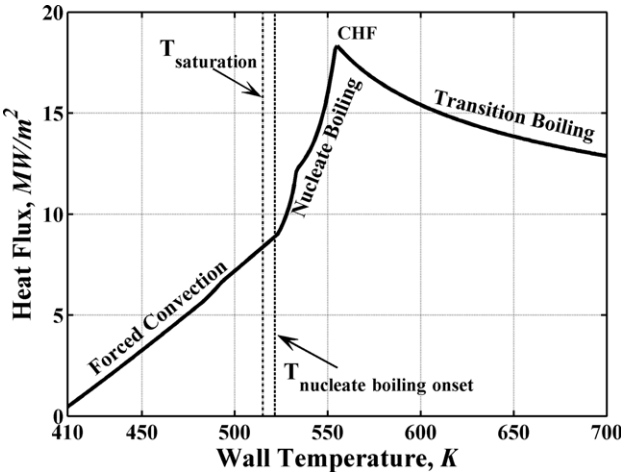

Figure 1. Heat flux to coolant with smooth tube as a function of wall temperature. Coolant conditions: bulk water temperature of 403 K, pressure of 3.5 MPa and water flow velocity of 10 m s^{-1}.

Two sets of correlations were employed to model the heat transfer from the coolant wall to the smooth channel with sub-cooled water.

The heat flux in the case of forced convection is determined by

$$q_{\mathrm{conv}} = \alpha_{\mathrm{conv}}(T_{\mathrm{w}} - T_{\mathrm{b}}), \quad (4)$$

where T_{b} is the bulk water temperature in the coolant and α_{conv} is the heat transfer coefficient.

Usually turbulent liquid flow is realized to get a high heat transfer coefficient. Therefore, the Dittus–Boelter [11] and Sieder–Tate [12] equations of a fully developed turbulent flow inside a smooth round tube were implemented. The Dittus–Boelter correlation for the heat transfer coefficient is given by

$$Nu = \frac{\alpha_{\mathrm{conv}}d_{\mathrm{h}}}{\kappa} = 0.023Re^{0.8}\mathrm{Pr}^{n}, \quad (5)$$

where the tubular Reynolds number is determined as $Re = Gd_{\mathrm{h}}/\mu_{\mathrm{b}}$; Prandtl number is $\mathrm{Pr} = c_p\mu_{\mathrm{b}}/\kappa$; G is the coolant mass velocity; d_{h} is the hydraulic diameter; μ_{b} is the bulk water dynamic viscosity; c_p is the specific heat at constant pressure and κ is the thermal conductivity. The exponent in the Prandtl number can vary: $n = 0.3$ for $T_{\mathrm{w}} < T_{\mathrm{b}}$ and $n = 0.4$ for $T_{\mathrm{w}} > T_{\mathrm{b}}$.

The Sieder and Tate correlation for the heat transfer coefficient is given by

$$Nu = \frac{\alpha_{\mathrm{conv}}d_{\mathrm{h}}}{\kappa} = 0.027Re^{0.8}\mathrm{Pr}^{1/3}\left(\frac{\mu_{\mathrm{b}}}{\mu_{\mathrm{w}}}\right)^{0.14}, \quad (6)$$

where μ_{w} is the water dynamic viscosity at the wall.

This correlation takes into account the variation in water properties from the bulk temperature to the wall temperature.

The above correlations described the processes of convective heat transfer in smooth tubes, which have the lowest efficiency from known channel configurations [13]. Swirl tape insert in the tube is one of the methods to enhance heat transfer

efficiency [14]. To consider heat sink in the swirl tube and to study the influence of such improvement on the structural stability of PFC at high thermal load, the following Marshall's modification of Sieder and Tate correlation was implemented:

$$Nu = \frac{\alpha_{\text{conv}} d_{\text{h}}}{\kappa} = 0.027 Re^{0.8} \text{Pr}^{1/3} \left(\frac{\mu_{\text{b}}}{\mu_{\text{w}}}\right)^{0.14} (3.2092 Y^{-0.248}), \tag{7}$$

where Y is the swirl tape twist ratio.

The bulk water temperature along the tube is determined from the time-dependent thermal balance equation:

$$T_{\text{b}}(y,t) = T_{\text{in}} + \frac{2\int_0^y q(y,t)\,\text{d}y}{c_p r G}, \tag{8}$$

where T_{in} is the inlet temperature in the coolant; r is the coolant tube radius and y is the distance along the tube.

The heat exchange in the case of nucleate boiling is determined by

$$q_{\text{b}} = \alpha_{\text{b}}(T_{\text{w}} - T_{\text{sat}}). \tag{9}$$

Two correlations—Thom *et al* [15] and Araki *et al* [16]—were implemented to calculate the heat transfer coefficient for a fully developed nucleate boiling regime.

The heat transfer coefficient in the case of Thom's correlation is given by

$$\alpha_{\text{b}} = \frac{10^6 (T_{\text{w}} - T_{\text{sat}}) \exp(2P/8.69)}{(22.65)^2}, \tag{10}$$

where P is water pressure in MPa.

Thom correlation was obtained for uniform heating conditions. The heat flux to the coolant channel in the fusion reactor is one-sided. Araki *et al* [16] proposed the following correlation for the fully developed nucleate boiling regime in the case of one-sided heating based on their experiments:

$$\alpha_{\text{b}} = \frac{10^6 (T_{\text{w}} - T_{\text{sat}})^2 \exp(3P/8.6)}{(25.72)^3}. \tag{11}$$

For regimes where the heat transfer to the coolant is determined by forced convection and nucleate boiling at the wall surface, Bergles and Rohsenow [17] proposed the following correlation:

$$q = q_{\text{conv}} \left[1 + \left\{\frac{q_{\text{b}}}{q_{\text{conv}}}\left(1 - \frac{q_{\text{i}}}{q_{\text{b}}}\right)\right\}^2\right]^{1/2}, \tag{12}$$

where q_{i} is the boiling heat flux at the point of incipient boiling.

A correlation for boiling incipience was also proposed by Bergles and Rohsenow. To start the nucleate boiling process, wall temperature has to exceed the saturation temperature by a certain value ΔT, and the heat flux q_{i} to the coolant in this case is given by

$$q_{\text{i}} = 1082 P^{1.156} \left(\frac{T_{\text{w}} - T_{\text{sat}}}{0.556}\right)^{\frac{2.1598}{p^{0.0234}}}. \tag{13}$$

At the same time this heat flux is equal to that derived from the wall to the coolant by forced convection. From this equality, using the last equations (13) and (4), it is then possible to calculate wall temperature T_{w} at the boiling incipient point. The boiling heat flux at this point is determined by substituting T_{w} in equation (9).

The above-stated calculation method of heat transfer to the coolant channel is correct only if the heat flux does not exceed the CHF value. If heat flux, however, at a certain location of the channel exceeds the critical value, the heat exchange in this place is reduced and must be described by other formula.

Tong [18] proposed the following correlation for the CHF calculation in smooth tube

$$q_{\text{CHF}} = 0.23 f_0 G H_{\text{fg}} \left(1 + 0.00216 \left(\frac{P}{P_{\text{c}}}\right)^{1.8} Re^{0.5} Ja\right), \tag{14}$$

where f_0 is the fanning friction factor, $f_0 = 8Re^{-0.6} \times (d_{\text{h}}/d_0)^{0.32}$; Ja is the Jakob number, $Ja = -\chi(\rho_{\text{l}}/\rho_{\text{v}})$; χ is the quality of sub-cooled liquid bulk, $\chi = -c_p(T_{\text{sat}} - T_{\text{b}})/H_{\text{fg}}$; H_{fg} is the latent heat of vaporization of water; P is the water pressure in the coolant; P_{c} is the critical pressure of water, $P_{\text{c}} = 22.089$ MPa; d_0 is the reference diameter, $d_0 = 0.0127$ m; ρ_{l} is the density of liquid bulk and ρ_{v} is the density of vapour at the saturation temperature.

Insert of swirl tape in the tube increases the flow speed near the channel wall and enhances mixing of fluid from the core with fluid in the wall. These processes enhance the efficiency in convective heat transfer and raise the value of CHF. Marshall's modification [19] for CHF in the case of the swirl tube takes into account the swirl tape twist ratio and the tape thickness:

$$q_{\text{CHF}} = 0.23 f_{\text{sw}} G H_{\text{fg}} \left(1 + 0.00216 \left(\frac{P}{P_{\text{c}}}\right)^{1.8} Re_{\text{sw}}^{0.5} Ja\right), \tag{15}$$

where friction factor for the swirl tape tube is determined as

$$f_{\text{sw}} = 8.0 Re_{\text{sw}}^{-0.6} \left(\frac{d_{\text{sw}}}{d_0}\right)^{0.32} 2.6125 Y^{-0.406}, \tag{16}$$

where the hydraulic diameter of the swirl tube $d_{\text{sw}} = (\pi d^2 - 4\delta d)/(\pi d + 2d - 2\delta)$ is used for calculation of the Reynolds number Re_{sw}, d is the inside diameter of the tube and δ is the tape thickness.

In our developed model the CHF value is determined at each time step. This value is time-dependent and location-dependent along the tube according to the water properties in the coolant channel. If the heat flux value to the coolant, calculated with correlations for forced convection and nucleate boiling, exceeds the CHF, then the heat flux at this channel location is calculated using Marshall [19] correlation in the following way:

$$q = q_{\text{CHF}} \left(\frac{T_{\text{w}} - T_{\text{sat}}}{T_{\text{CHF}} - T_{\text{sat}}}\right)^{-0.23}, \tag{17}$$

where T_{CHF} is the local wall temperature at the moment of achieving the CHF value.

5. Validations and benchmarking

Several experiments from various sources [20–23] were used to benchmark our numerical simulation to validate the developed

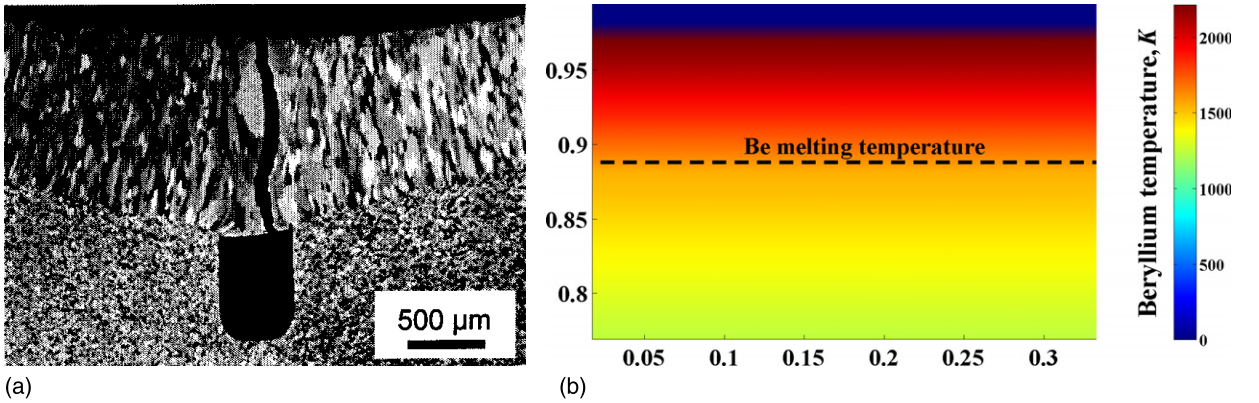

Figure 2. Melt layer behaviour during VDEs (deposited energy density 60 MJ m^{-2} in 1.5 s). Divertor module experiment micrograph [20] and HEIGHTS simulation result.

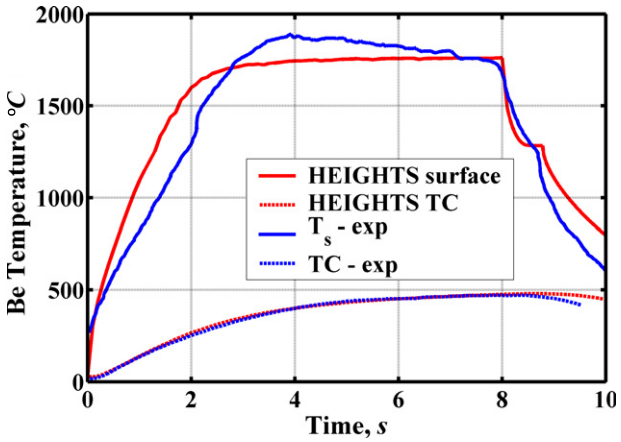

Figure 3. 10 mm thick Be armour response at surface and at thermocouples location.

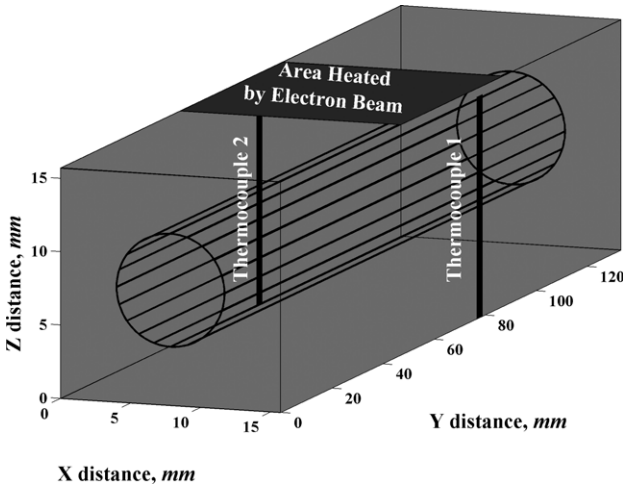

Figure 4. Schematic illustration of the experimental mockup.

model implemented in HEIGHTS before applying it to ITER-like simulation.

The first benchmark is an experiment performed in the electron beam facility JUDITH [20]. In this experiment a divertor module FT38/2 with Be armour on CuCrZr structure was exposed in conditions equivalent to VDE with deposited surface energy of 60 MJ m^{-2} within 1.5 s. The processes of energy deposition, heat conduction in Be, melting and vaporization of Be were modelled and compared with the above experiment. Figure 2(*a*) shows a cross-section of the exposed Be target after the energy deposition [20]. Figure 2(*b*) shows the HEIGHTS simulation results for the same conditions. Graphical and numerical comparison of both the experimental data and the simulation results showed very good agreement with both the vaporized and the melted thickness of Be. This demonstrates confidence in our heat conduction, phase change and vaporization models.

Several sets of experiments performed in the JET Beryllium test [21] were also used to benchmark the time-dependent surface temperature behaviour and temperatures at thermocouples located 10 mm below the exposed surface. Modelling of long-time, 7 and 8 s, energy deposition with various intensities showed good agreement with the measured experimental data, especially in cases where the Be surface temperature was above the liquidus temperature [21]. Figure 3 shows a comparative analysis of the Be armour response of 20 MW m^{-2} energy impact within 8 s. A slight difference in the shape of surface temperature curves is explained by deviations in the power density profiles. We modelled the square beam pulse.

Several experiments using one-sided heating of the mockup by an electron beam [22] were extensively simulated for benchmarking models of heat transfer to coolant channels. The mockup was made of an oxygen-free high-conductivity copper (OFHC-Cu) bar stock with an axially centred circular coolant channel. Two thermocouples (TC-1 and TC-2) were placed on each side of the heated area, symmetric relative to the tube cross-section as schematically illustrated in figure 4. The thermocouples coordinates are specified as 8 mm before the exit of the heated length and at 0.6 mm below the surface. The first part of the experiments was aimed at achieving steady-state conditions. These processes were simulated for different values of the incident heat flux (IHF), water temperature in the channel inlet, pressure and velocity in the channel. The IHF was varied from 3.5 to 14.6 MW m^{-2}, the inlet water temperature was varied from 10 to 69 °C, and the water velocity was varied from 1 to 10.2 m s^{-1}. The measured parameters are the temperature in both thermocouple locations at TC-1 and TC-2, and water temperature at the exit from the tube.

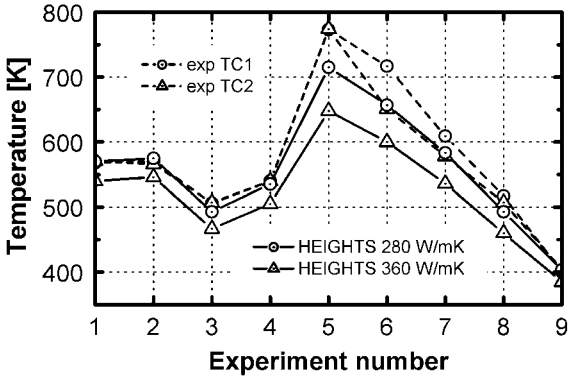

Figure 5. Copper temperature at thermocouples location under steady-state heat loading for different values of IHF, flow velocity and water inlet temperature.

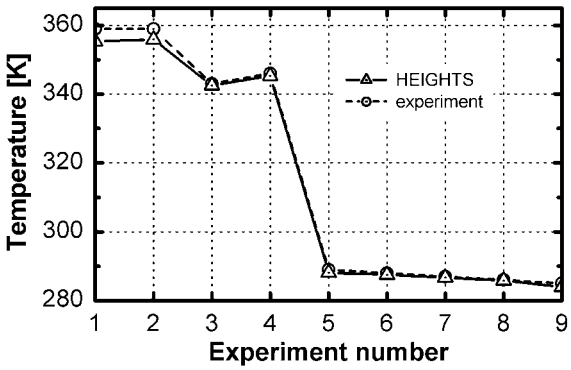

Figure 6. Water outlet temperature under steady-state heat loading for different values of IHF, flow velocity and water inlet temperature.

As shown in figure 5, numerical simulation results agree well with the experimental data using the OFHC-Cu thermal conductivity of 280 W m^{-1} K^{-1}. There is a slight difference in the reading of the supposed to be two identical thermocouples TC-1 and -2. The experiment number in figure 5 corresponds to the shot number in the data table of experiments [22]. A comparison between HEIGHTS calculated and measured water outlet temperatures is shown in figure 6. A slight deviation from the experiment is observed for regimes with low flow velocity (1 m s^{-1}). This could be due to the limitation of the correlations used for the Reynolds and Prandtl numbers for the forced convection. The Sieder and Tate correlation for turbulent flows is acceptable for Reynolds numbers $>10^4$. In our case Re $\sim 1.7 \times 10^4$ for velocity 1 m s^{-1}, that is, near the boundary limit for the correct use of the above correlation.

The next set of experiments modelled the processes of the loss-of-flow accident (LOFA) in the coolant channels. In these experiments the water flow loop's circulation pump was disabled after the steady-state condition was achieved. This resulted in an almost linear decrease in the coolant flow velocity down to 0 m s^{-1} in a duration of ~8 s. This mockup was heated by the electron beam with the same intensity. The temperature change was controlled by the thermocouple. When the temperature at the thermocouple location reached 700 °C the electron beam heating was discontinued. The purpose of these experiments was to determine the time between the start of flow velocity decrease and the mockup heating up to the above temperature. It is mockup time-to-burnout (TBO), which characterizes mockup's survivability. In our HEIGHTS simulation we took into account the linear velocity decrease that affected both the forced convective heat transfer and the CHF value. The CHF specified by the thermocouple position along the tube is reduced with time from ~8 MW m^{-2} to ~80 KW m^{-2} as a result of velocity decrease and water bulk temperature increase. This low value of the CHF fully determines local heat transfer from the coolant wall and is responsible for the increase in temperature at the thermocouple. Figure 7 shows excellent agreement of our HEIGHTS simulation results of the thermocouple temperature rise compared with the experimental data. Other codes and models were not able to reproduce such agreement [22].

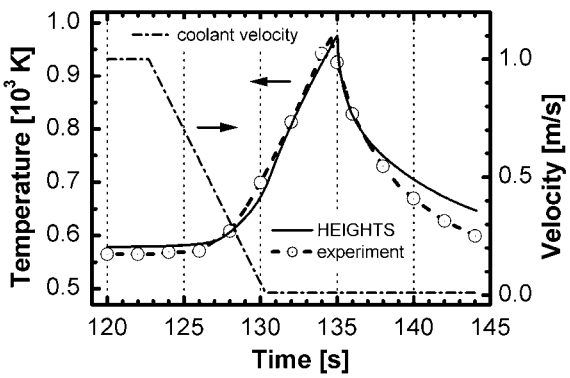

Figure 7. HEIGHTS modelling of LOFA and comparison with experimental data [2].

HEIGHTS also modelled heat transfer processes in tubes with swirl tape insert. Models include modified correlations for convective heat transfer and CHF. Experimental data from round robin CHF testing [23] were used for validation of these modifications. The experimental mockup was made from Glidcop Al-25 with coolant channel located 2 mm beneath the heated area. The coolant channel had 10 mm internal diameter and included swirl tape with a thickness of 2 mm and a twist ratio of 2. The two thermocouples registered temperatures at 2.2 and 7.2 mm distances from the heated surface. The surface temperature was additionally measured. The water flow in the coolant tube had 12 m s^{-1} velocity, 3.5 MPa inlet pressure and 117 °C inlet temperature. We modelled experiments using a uniform heat flux profile and with intensities varying from 5 to 30 MW m^{-2} (figure 8). Steady-state operation of the above described mockup with the given coolant parameters is possible for a maximum surface heating of around 26 MW m^{-2}. At higher energy densities the heat flux to the coolant exceeds the CHF value that leads to an increase in wall temperature with time and following burnout. HEIGHTS simulation results are in very good agreement with the experimental data up to the incident critical heat flux (ICHF) value of ~27 MW m^{-2}.

6. VDE simulation in ITER-like devices

The detailed models of heat transfer in the structural materials described above, especially the accurate description of the heat transfer to the coolant are most important in the simulation of long-duration heating processes such as steady-state heat loading or during plasma transient VDE. While modelling the

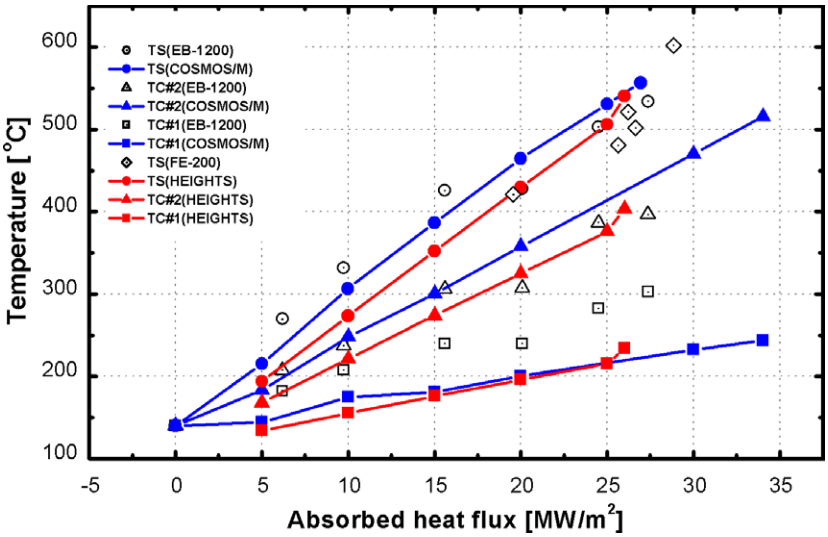

Figure 8. Experiments and simulation of CHF testing in tube with twist tape insert.

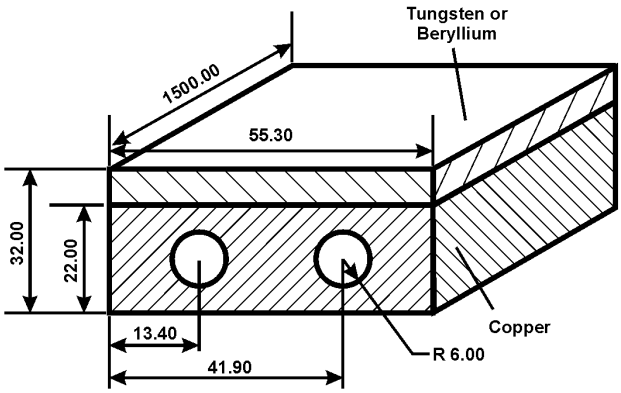

Figure 9. Schematic illustration of a ITER-like divertor module design.

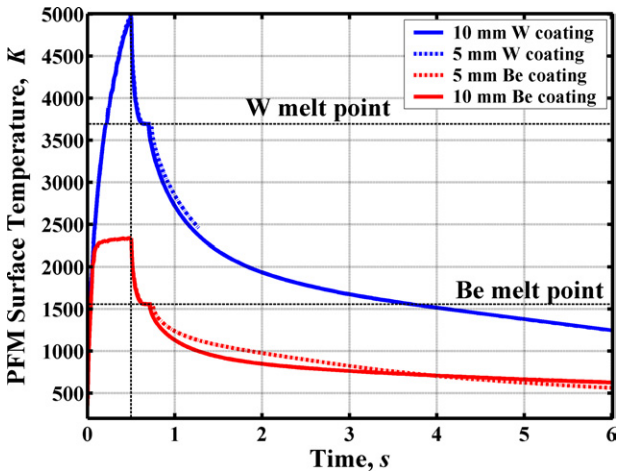

Figure 10. Surface temperature of coating materials for 0.5 s deposition time.

steady-state heating is interesting for a parametric study of this condition, examination of system response during VDE is of critical importance as such regimes can cause severe surface melting, surface erosion and substantially damage the structural components of the reactor. An additional concern is the higher temperature in the structural material, particularly at the interface with the coating materials. Elevated temperatures will seriously degrade the interface bonding and cause detachment of the coating from the structural material.

ITER-like structure compositions, sizes and coolant parameters were analysed using our VDE models with plasma energy density of 60 MJ m^{-2} deposited over 0.5 s. A typical design of plasma facing and structural materials is schematically shown in figure 9. The structural material is copper coated by tungsten or beryllium with water being the coolant. Figure 9 also shows the actual design dimensions given in millimetres for an entire ITER-like module that would be exposed to a VDE.

The length of the simulated ITER-like module is 1.5 m with an inlet pressure of 3.6 MPa. While the insignificant pressure loss in a smooth tube is not so important for heat exchange, the pressure drop along the channels with swirl tape insert can influence the heat transfer. Therefore, we take into account the changing of this value for swirl tubes. The water flow velocity and water temperature at the inlet were varied.

Recent modelling of the VDE heat loading in copper structure with 5 and 10 mm thick beryllium coatings demonstrates full protection of the copper substrate due to the low-z Be material [2]. Most of the incident plasma energy is removed by beryllium's higher surface vaporization rate, leaving little energy to be conducted through the structural material that does not cause melting at the Be/Cu interface.

The thermal response of both Be and W coated modules of PFC is shown in figure 10 for standard VDE parameters of 60 MJ m^{-2} plasma deposited energy in 0.5 s duration. Both Be and W exhibit significant melting while Be shows much more vaporization thickness than W, as shown in figure 11. The large vaporization thickness of the Be module and the energy removed as a result will then cause less damage to the copper structure, as will be shown later. Figure 12 shows the effect of shorter VDE deposition time on W module. The shorter VDE time of 0.2 s results in significant surface vaporization of W compared with the 0.5 s deposition time.

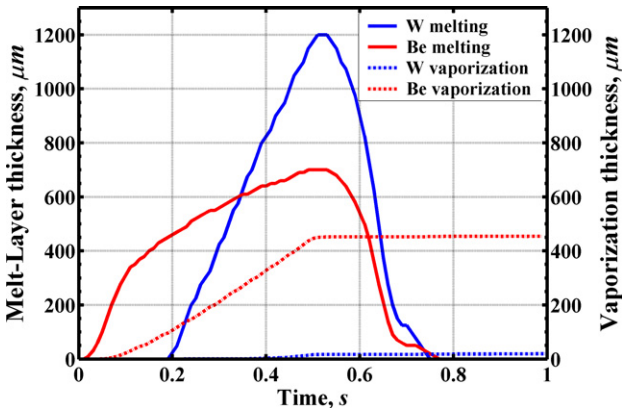

Figure 11. Melting and vaporization layer of 5 mm W and Be armour for 0.5 s deposition time.

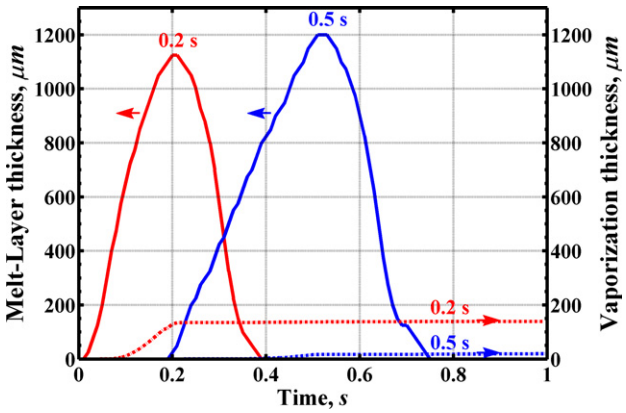

Figure 12. Melting and vaporization layer of 5 mm W armour for 0.2 and 0.5 s deposition time.

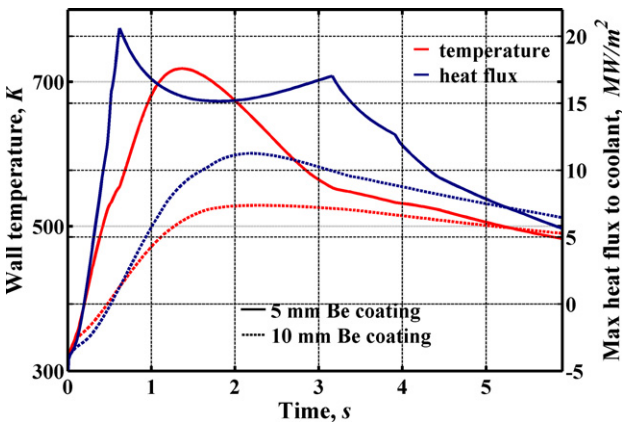

Figure 13. Coolant wall temperatures and corresponding boiling curves for structures with 5 and 10 mm Be coating (inlet water temperature of 413 K, water flow velocity of 20 m s^{-1}).

The results of the HEIGHTS simulation of VDE heat loading in Cu structures with different thicknesses of Be armour demonstrate the interdependence of coolant wall temperature and heat exchange processes between the wall and the sub-cooled water as shown in figure 13. In the case of 10 mm Be coating practically all the heat flux from the channel wall is carried away only by forced convection in the coolant. Wall temperature reaches the value at which the

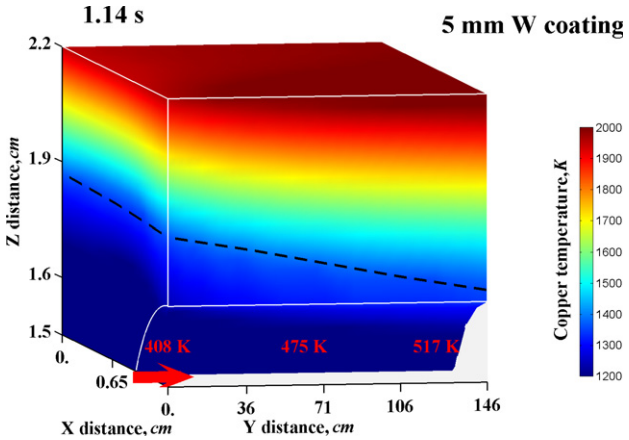

Figure 14. Copper mockup temperature under 5 mm W coating (inlet water temperature of 403 K, water flow velocity of 12 m s^{-1}). Red numbers show bulk temperature along channel. The dotted line indicates copper melt layer.

process of nucleation near the wall begins but fully developed nucleate boiling at the wall does not take place in this situation. However, in the case of 5 mm Be coating the channel wall temperatures are much higher. At the beginning heat transfer to the coolant is provided by forced convection, then by both forced convection and nucleate boiling. When the local heat flux to the coolant exceeds the corresponding CHF value (which depends on coolant velocity, temperature and pressure), heat transfer to the water coolant at this wall location is reduced and therefore causes wall temperature increase. Eventually, the thermal load from the surface decays and therefore the wall temperature is decreased. So, the value of heat transfer to the coolant is increased slightly since the regime of exceeding CHF depends additionally on wall temperature. When wall temperatures reach values at which heat flux to the water is lower than CHF, heat exchange is again controlled by both forced convection and nucleate boiling.

Full 3D simulation allows a detailed analysis of the structure across and along the coolant channels. Our models also take into account changing of the flow temperature along the tube. While in the case of moderate heat flux from the wall, a little increase in the water temperature at the end of the tube does not influence much the heat exchange processes, higher thermal load from the wall along the channel can significantly increase the water bulk temperature and impair the water condition from being a better heat transfer media at the outlet. More obviously, this situation appears in the case of 5 mm W coating and especially in channels with swirl tape insert. Figure 14 shows copper and water bulk temperatures along the tube at the start of coolant wall melting. The high heat flux from the wall along tube causes a rise in the bulk temperature at the outlet of up to ~430 K at the moment of exceeding the CHF. Therefore, the CHF value at the end of the tube is much lower than at the inlet. This influences the decrease in possible heat transfer value and as a result the rapid increasing of wall temperature. Figure 15 shows the time dependence of the CHF values and the heat flux to the coolant at the top of the coolant tube. We did not consider in this particular numerical simulation the steady-state condition of the mockup and started our simulation from the initial temperatures of

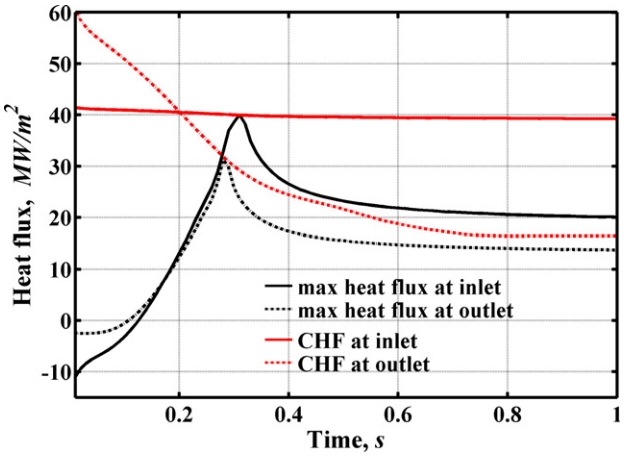

Figure 15. Heat flux to coolant at the inlet and at the outlet (inlet water temperature of 403 K, water flow velocity of 12 m s^{-1}).

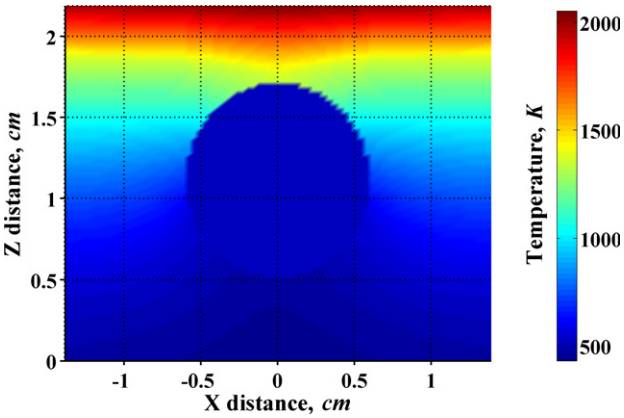

Figure 16. Cross-sectional temperature distribution of copper mockup under 5 mm W coating.

structural materials of 300 K. Therefore, water heated the copper wall at the beginning since the inlet water temperature was 403 K. The critical flux values at the inlet and outlet differ significantly, which determines the differences in the resulting heat exchange and wall temperatures. Exceeding the CHF also explains cross-sectional temperature distributions where the temperature at the tube area is higher than at the edge of the mockup (figure 16). As the heat transfer to the coolant channel is reduced, increasing local wall temperature is spread around and along the tube.

Numerical simulation of VDE was conducted to compare tungsten and beryllium since these materials are considered plasma facing components in the ITER device (figure 17). Results indicated that tungsten coating of 5 mm thickness cannot protect the heat sink material under typical VDE heat loading. The copper layer is melted completely right up to inside of the coolant channels. In the case of 10 mm W coating, melting at the W/Cu interface will cause significant degradation at the interface of these materials. As shown in figure 18, safer operation of the copper structure is possible with W armour of 15 mm thickness or larger.

In view of the above considerations we studied the dependence of copper layer temperatures on tungsten coating thickness for channels with smooth and swirl tubes.

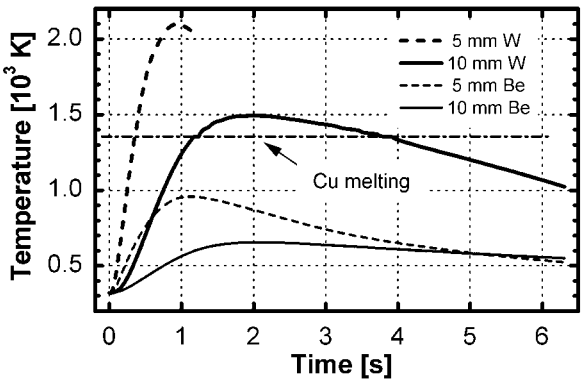

Figure 17. Copper surface temperature under 5 or 10 mm coating of W or Be [2].

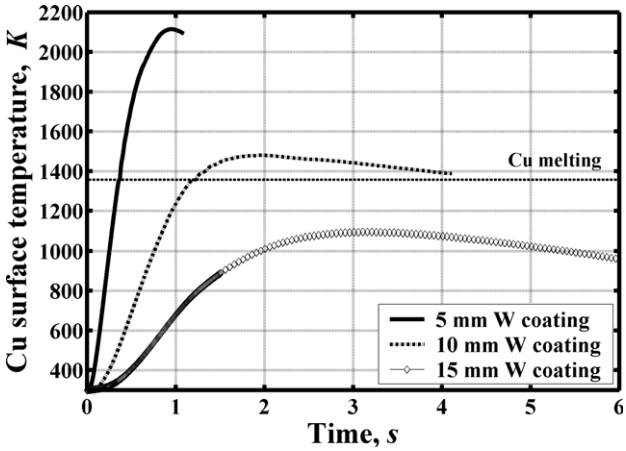

Figure 18. Copper surface temperature under 5, 10 and 15 mm coating of W.

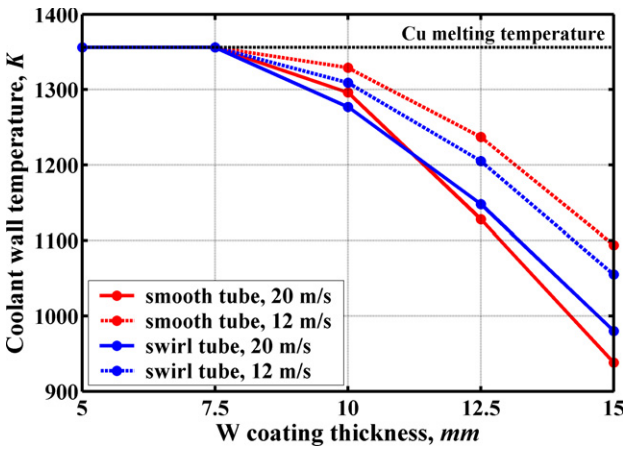

Figure 19. Coolant wall temperatures in dependence on tungsten layer thickness for smooth tube and tube with swirl tape insert (inlet water temperature of 403 K).

Enhancement of coolant parameters, such as swirl tape insert or increasing flow velocity, changes little the coolant wall temperatures (figure 19), but does not influence much the copper surface temperature behaviour (figure 20).

Insertion of twisted tape in coolant tubes may enhance the heat-removing capability. However this enhancement

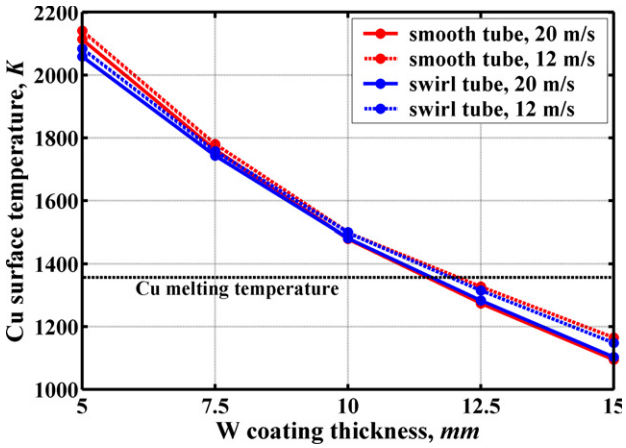

Figure 20. Copper surface temperatures in dependence on tungsten layer thickness for smooth tube and tube with swirl tape insert (inlet water temperature of 403 K).

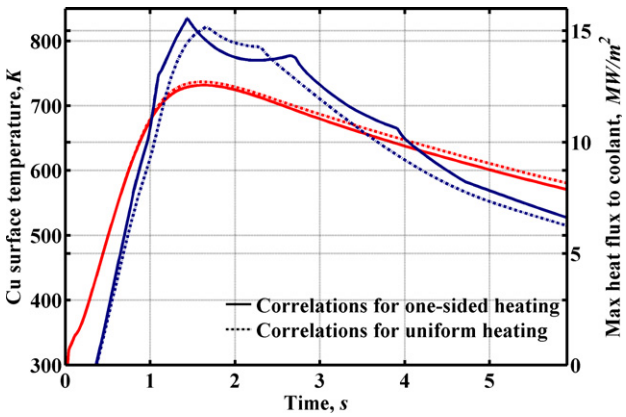

Figure 21. Comparison of correlations for one-sided and uniform heating. Boiling curves (blue) and corresponding copper surface temperatures (red) in structure with 8 mm Be coating (inlet water temperature of 413 K, water flow velocity of 20 m s^{-1}).

increases the heat transfer to the coolant along the whole tube. As a result, the water flow reaches the outlet with a much higher bulk temperature than at the inlet if we consider ITER-actual length of ∼1.5 m channel. This reduces the efficiency of the swirl tube near the end of the channel. Only a thicker tungsten layer can reduce the heat flux intensity reaching the copper structure and correspondingly the coolant channel wall. In these cases low thermal load to the wall allows a safe regime of heat sink to the sub-cooled water.

Our model contains two sets of correlations for heat transfer by forced convection and nucleate boiling. One set is intended for uniform channel heating (fission-like conditions) and the second is for one-sided heating (fusion-like conditions). This is intended to highlight the importance of using the correct heat transfer correlations and benchmarking more relevant experimental data. To study the effect of these sets on temperature values in the structural materials, numerical simulations with the same input parameters for both correlations were conducted. We obtained different temperatures for the channel wall and slightly different temperature for the copper surface. Figure 21 shows that the heat transfer values at the top of the tube are higher with one-sided correlations, except for periods exceeding the CHF. However, such a difference does not have a large influence on the temperature of the copper surface in the divertor module.

7. Conclusion

HEIGHTS full 3D models were developed and enhanced to study the behaviour of plasma facing and structural materials during longer plasma transient events. The models include detailed plasma energy deposition on PFMs, thermal conduction processes, coating and structural material phase changes, coating materials evaporation and thermal hydraulics of coolant tubes. Processes of heat transfer to coolant as results of forced convection and sub-cooled boiling were also modelled for both smooth and twisted tape coolant channels. Time and spatial dependence of changes in water properties are taken into account when the heat transfer coefficient and CHF are calculated. The HEIGHTS package was benchmarked against several known laboratory data and showed excellent agreement in the simulation of both coating material erosion and melt layer thicknesses for VDE transient conditions and structural material response of copper mockup for steady-state condition as well as for LOFA and CHF criteria in smooth and swirl tubes.

The thermal response of ITER-like design modules to plasma VDE was studied in detail. Results of plasma energy transient deposition of 60 MJ m^{-2} over 0.5 s indicate that if the copper structure is covered by 5–10 mm tungsten or 5 mm beryllium, the heat flux to the coolant channels achieves the critical value. HEIGHTS results also showed that Be coating significantly decreases the flow of incident plasma energy to the copper layer and prevents copper melting even in the case of 5 mm thickness where local CHF was achieved. This is simply because of the large fraction of the incident energy removed by the extensive Be vaporization. Tungsten coating removes less plasma energy by surface vaporization and therefore only the thicker W layers—⩾15 mm—allow reduction of the heat flux intensity to sink material to ensure safe operation of copper and coolant channels. Changing of coolant hydraulic parameters has little impact on copper temperatures behaviour in the cases studied.

Acknowledgment

This work is supported by the US Department of Energy, Office of Fusion Energy Sciences.

References

[1] Hassanein A. 2002 *Fusion Eng. Des.* **60** 527
[2] Hassanein A., Sizyuk T. and Ulrickson M. 2008 Vertical displacement events: a serious concern in future ITER operation *Fusion Eng. Des.* at press
[3] Hassanein A. 1996 *Fusion Technol.* **30** 713
[4] Raffray A.R. and Federici G. 1997 *J. Nucl. Mater.* **244** 85
[5] Hassanein A., Federici G., Konkashbaev I., Zhitlukhin A. and Litunovsky V. 1998 *Fusion Eng. Des.* **39–40** 201
[6] Hassanein A. 1988 Response of materials to high heat fluxes during operation in fusion reactors *ASME* 88-WA/NE-2
[7] Kandlikar S.G. 2001 *Multiph. Sci. Technol.* **13** 207

[8] Hassanein A., Kulcinski G.L. and Wolfer W.G. 1984 *Nucl. Eng. Des./Fusion* **1** 307
[9] Hassanein A. 1984 *J. Nucl. Mater.* **122–123** 1453
[10] Jouhara H.I. and Axcell B.P. 2002 *Trans IChemE* **80** 284
[11] Dittus E.J. and Boelter L.M.K. 1930 *Publ. Eng.* **2** 443
Dittus E.J. and Boelter L.M.K. 1985 *Int. Commun. Heat Mass Transfer* **12** 3 (reprinted)
[12] Sieder E.N. and Tate G.E. 1936 *Indust. Eng.Chem.* **28** 1429
[13] Raffray A.R. *et al* 1999 Critical heat flux analysis and R and D for the design of ITER divertor *Fusion Eng. Des.* **45** 377
[14] Baxi C.B. 1995 Comparison of swirl tape and hypervapotron for cooling of ITER divertor *Proc. 16th IEEE/NPSS Symp. on Fusion Engineering (SOFE'95) (Champaign, IL, USA)* p 186
[15] Thom J.R.S. *et al* 1965–1966 *Proc. Inst. Mech. Eng.* **180** 226
[16] Araki M., Ogawa M., Kunugi T., Satoh K. and Suzuki S. 1996 *Int. J. Heat MassTransfer* **39** 3045
[17] Bergles A.E. and Rohsenow W.M. 1964 *Trans. Am. Soc. Mech. Eng.* **86** 365
[18] Tong L.S. 1975 ASME Paper, 75-HT-68
[19] Marshall T.D. 1998 Experimental examination of the post-critical heat flux and loss of flow accident phenomena for prototypical ITER divertor channels *Doctoral Thesis* Rensselaer Polytechnic Institute, Troy, New York
[20] Rodig M., Duwe R., Linke J., Qian R.H. and Schuster A. 1997 Degradation of plasma facing materials due to severe thermal shocks *17th IEEE/NPSS Symp. on Fusion Engineering (San Diego, CA, USA)* p 865
[21] Falter H.D., Ciric D., Godden D.J. and Ibbot C. 1997 High heat flux exposure tests on monoblocks brazed to a copper swirltube, JET–R(97)04, January 1997
[22] Marshall T.D., McDonald J.M., Cadwallader L.C. and Steiner D. 2000 *Fusion Technol.* **37** 38
[23] Youchison D.L., Schlosser J., Escourbiac F., Ezato K., Akiba M. and Baxi V.B. 1999 Round robin CHF testing of an ITER vertical target swirl tube *Proc. 18th IEEE/NPSS Symp. on Fusion Engineering (Albuquerque, NM, USA)* p 385